Supporting Information

Artificial Antibody Created by Conformational Reconstruction of the Complementary-Determining Region on Gold Nanoparticles

Gui-Hua Yan[a,1], Kun Wang[a,1], Zhuxue Shao[a,1], Lei Luo[a,1], Zheng-Mei Song[a], Jingqi Chen[a], Rong Jin[a], Xiaoyong Deng[a], Haifang Wang[a,2], Zhonglian Cao[b], Yuanfang Liu[a,c] and Aoneng Cao[a,2]

[a]*Institute of Nanochemistry and Nanobiology, Shanghai University, Shanghai 200444, China*

[b]*School of Pharmacy, Fudan University, Shanghai 201203, China*

[c]*Beijing National Laboratory for Molecular Sciences, College of Chemistry and Molecular Engineering, Peking University, Beijing 100871, China*

[1]*These authors contributed equally to this work.*

[2]*Corresponding authors: Aoneng Cao (ancao@shu.edu.cn) and Haifang Wang (hwang@shu.edu.cn)*

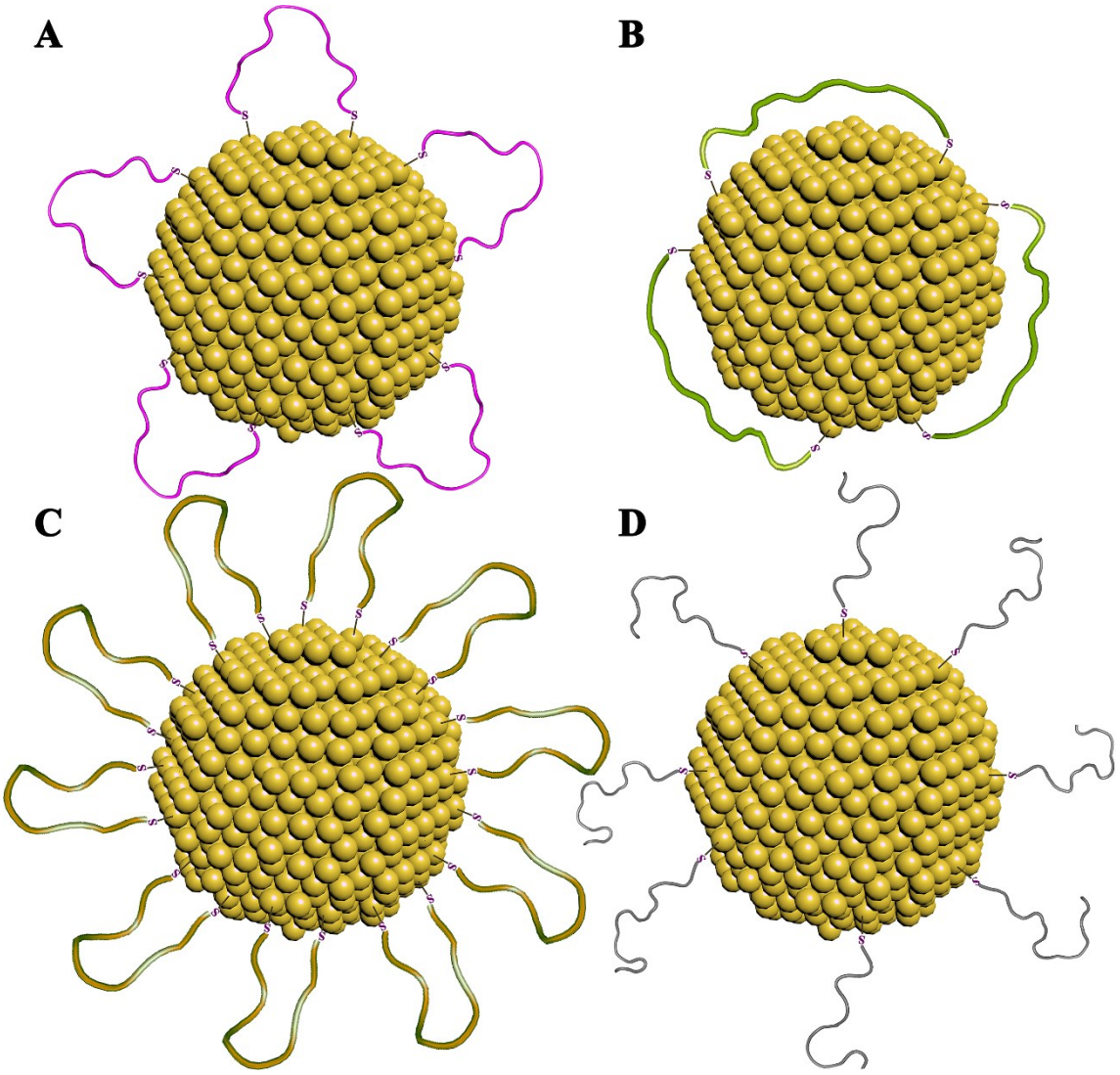

Fig. S1. Scheme of tuning the conformation of CDR peptides grafted onto AuNP by adjusting the peptide density. **(A)** Optimal peptide density on the surface of AuNPs results in suitable CDR conformation for binding (or small conformational space corresponding to the small red circle in **Fig. 1**). **(B)** Low peptide density results in extended peptide conformations (or larger conformational space corresponding to the magenta circle in **Fig. 1**). **(C)** High peptide density results in squeezed conformation (small conformational space likely corresponding to area between the red and magenta circles in **Fig. 1**). **(D)** One-point anchored peptides adopt random coil conformation (the largest conformational space corresponding to the whole cyan sheet in **Fig. 1**).

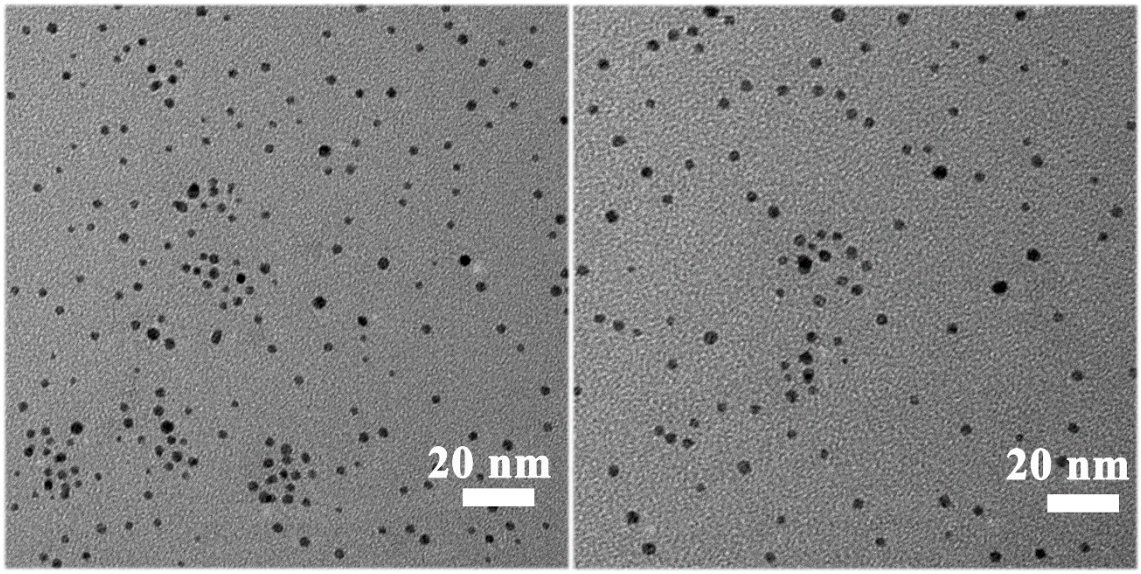

Fig. S2. HRTEM images of 3.6 nm non-functionalized AuNPs (left) and 3.6 nm AuNP-Pep (right), showing not apparent size difference due to the light atoms and small size of peptides.

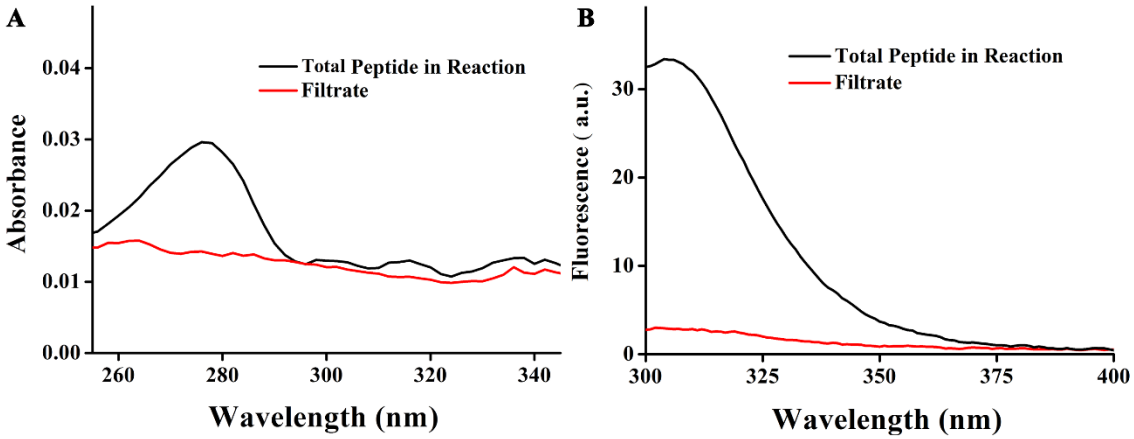

Fig. S3. The efficiency of peptide conjugation on AuNPs as determined by UV absorbance **(A)** and fluorescence **(B)** of the total peptides (black lines) and unreacted peptides (red lines). Both the absorbance peak at 280 nm and the fluorescence emission of Pep1 disappear, indicating nearly complete conjugation of Pep1 onto AuNPs.

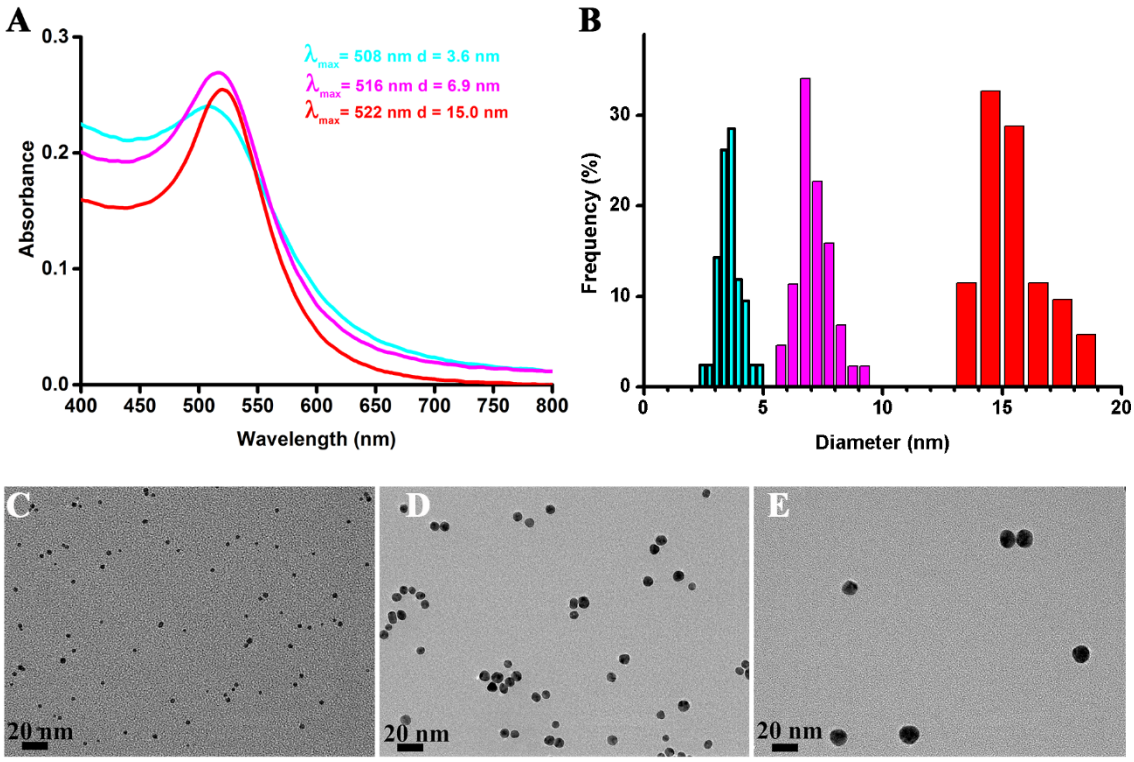

Fig. S4. Sizes of the three non-functionalized AuNPs characterized by HRTEM. **(A)** UV-Vis spectra of the three non-functionalized AuNPs**.** Their diameters were calculated to be 3.6 nm, 6.9 nm and 15.0 nm, respectively. **(B)** Size distributions of the three AuNPs counted from HRTEM images as represented by colorful histograms, with average sizes of 3.6±0.5 nm, 7.1±0.7 nm and 16.0±1.5 nm for **(C), (D)** and **(E)**, respectively.

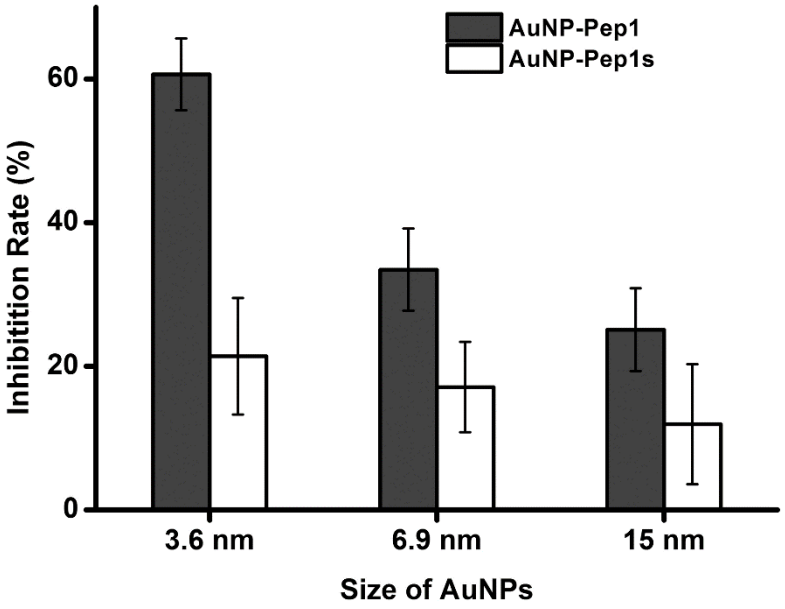

Fig. S5. Inhibition of the activity of 20 nM HEWL by different sized AuNPs functionalized with Pep1 or Pep1s with the same peptide density (one peptide per 0.68 nm^2 surface) on the AuNP surfaces. The concentrations for 3.6 nm AuNPs, 6.9 nm AuNPs and 15.0 nm AuNPs were 4.3 nM, 1.13 nM and 0.25 nM, respectively, therefore all samples have the same total number of peptide.

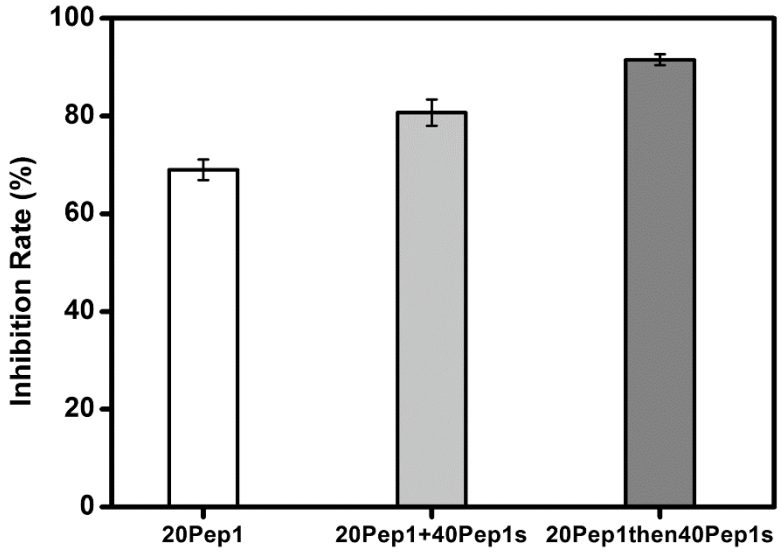

Fig. S6. Inhibition of the activity of HEWL by AuNP-Pep1 (3.6 nm). White, AuNP functionalized with 20 Pep1; light grey, AuNP functionalized with mixture of 20 Pep1 and 40 Pep1s; dark grey, AuNP first functionalized with 20 Pep1, and then 40 Pep1s was functionalized.

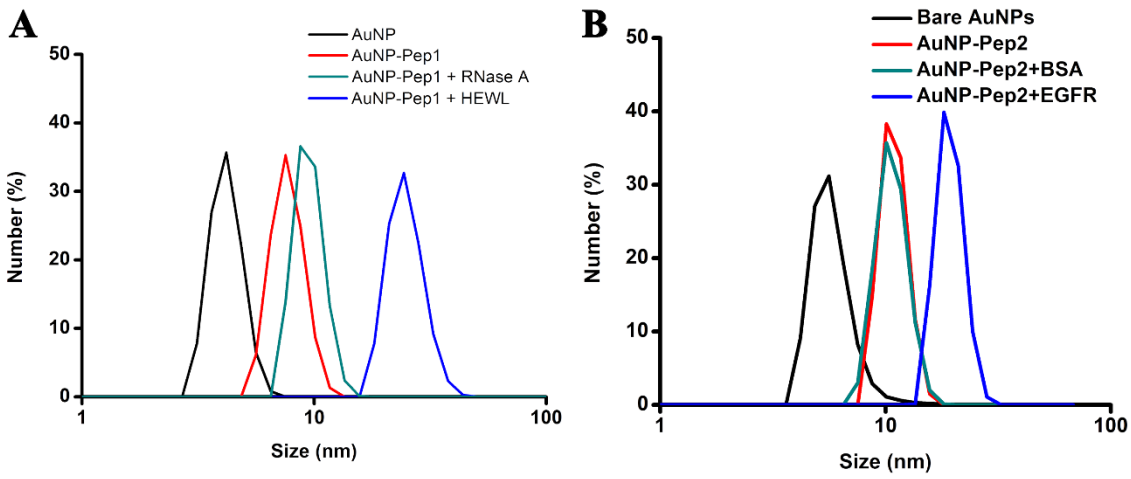

Fig. S7. Hydrodynamic diameter distribution of 3.6 nm AuNPs after peptide functionalization and interaction with proteins as measured by DLS. Functionalization with peptide increases the hydrodynamic diameter of AuNPs. **(A)** The big hydrodynamic diameter difference between the mixtures of AuNP-Pep1/HEWL and AuNP-Pep1/RNase A demonstrates the strong specific binding between AuNP-Pep1 and HEWL**. (B)** The big hydrodynamic diameter difference between the mixtures of AuNP-Pep2/EGFR and AuNP-Pep2/BSA demonstrates the strong specific binding between AuNP-Pep2 and EGFR.

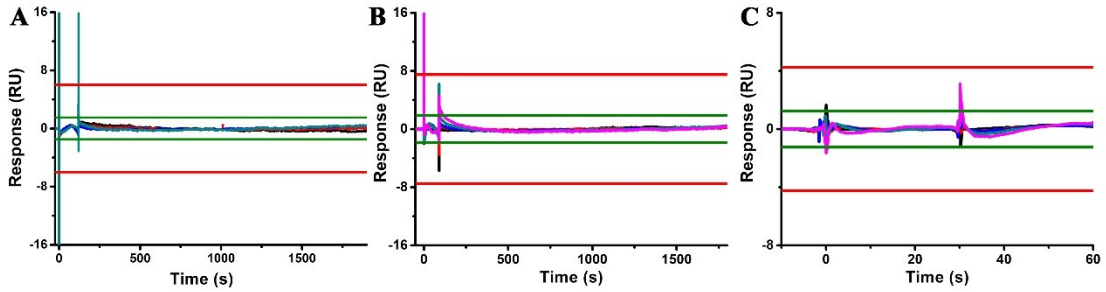

Fig. S8. Residue plots of SPR kinetic data fitting in this work. **(A)** Residue plot for the kinetics of the anti-lysozyme Goldbody binding to the immobilized HEWL (**Fig. 5*B*.** The chi^2 is 0.127, and the U-value is 2.). **(B)** Residue plot for the kinetics of the anti-EGFR Goldbody binding to the immobilized sEGFR (**Fig. 7*C*.** The chi^2 is 0.105, and the U-value is 2.). **(C)** Residue plot for the kinetics of EGF binding to the immobilized sEGFR **(Fig. 7*D*.** The chi^2 is 0.0306, and the U-value is 2.**)**. Green lines indicate 95% confidence intervals, and red lines indicate 90% confidence intervals.

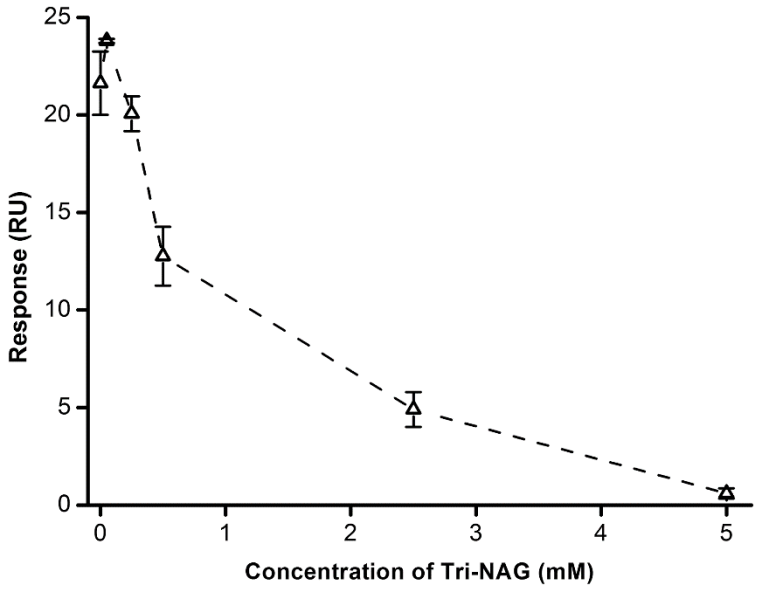

Fig. S9. SPR binding of AuNP-Pep1 to the immobilized HEWL on a CM5 chip as a function of Tri-NAG concentration.

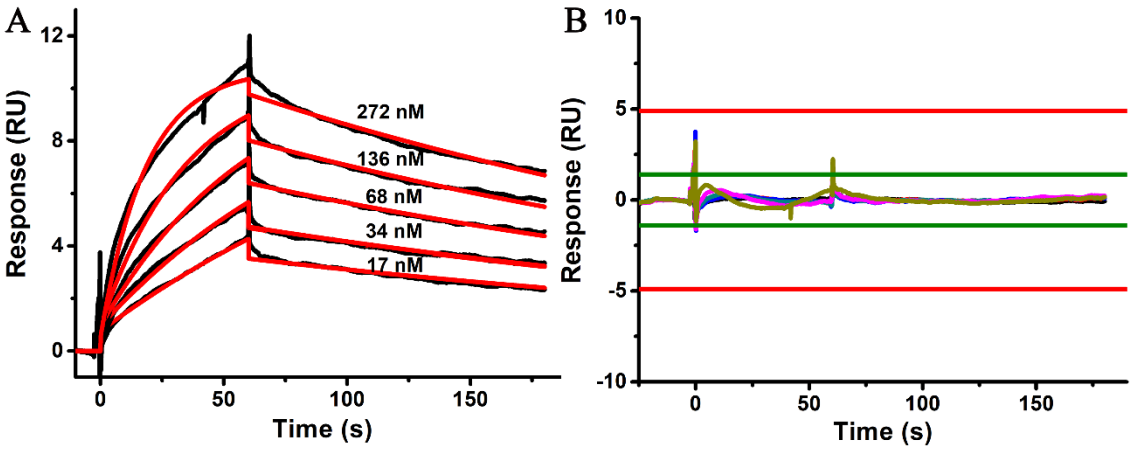

Fig. S10. SPR binding kinetics of the immobilized sEGFR with 17, 34, 68, 136 and 272 nM Cetuximab flowing through the chip. **(A)** Black curves are the experimental data, and red curves are the fitting lines. **(B)** Residue plot for the fitting (The chi^2 is 0.0433, and the U-value is 2.). Green lines indicate 95% confidence intervals, and red lines indicate 90% confidence intervals.

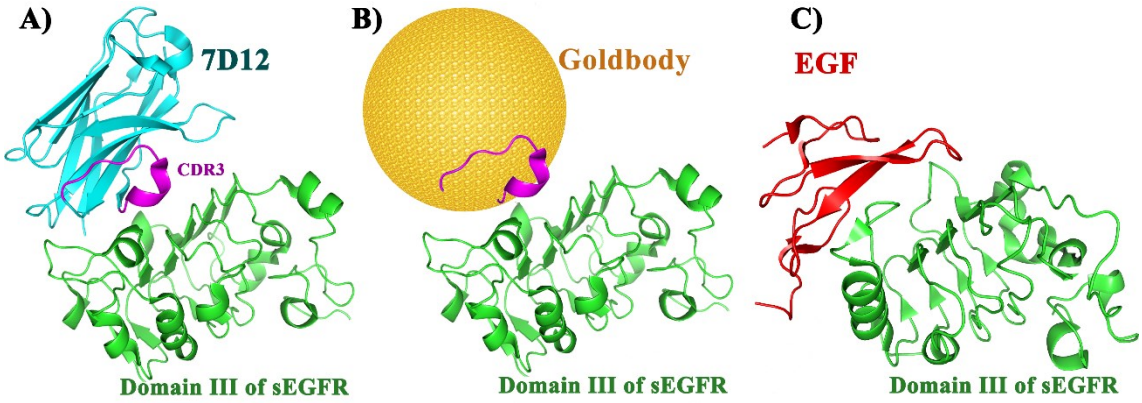

Fig. S11. Binding sites on the domain III of sEGFR for 7D12, anti-EGFR Goldbody, and EGF**. (A)** Structure of antibody 7D12 (cyan, with the CDR3 shown in magenta) in complex with the domain III of sEGFR (green) (PDB code: 4KRL). **(B)** Model of the anti-EGFR Goldbody (with the grafted peptide loop shown in magenta) in complex with the domain III of sEGFR (green). **(C)** Model of EGF (red) in complex with the domain III of sEGFR (green) (PDB code: 1IVO).

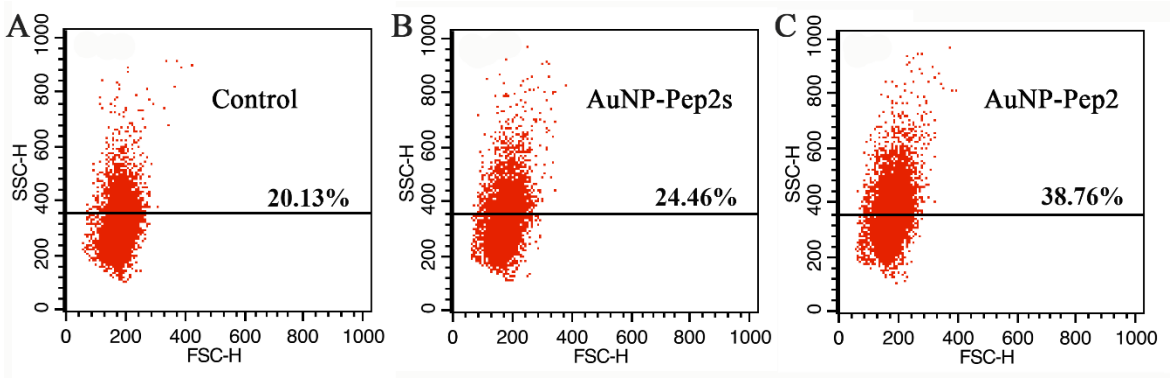

Fig. S12. Flow cytometry 2-D scatter plots of control cells, cells incubated with AuNP-Pep2s, and cells incubated with the anti-EGFR Goldbody, respectively.

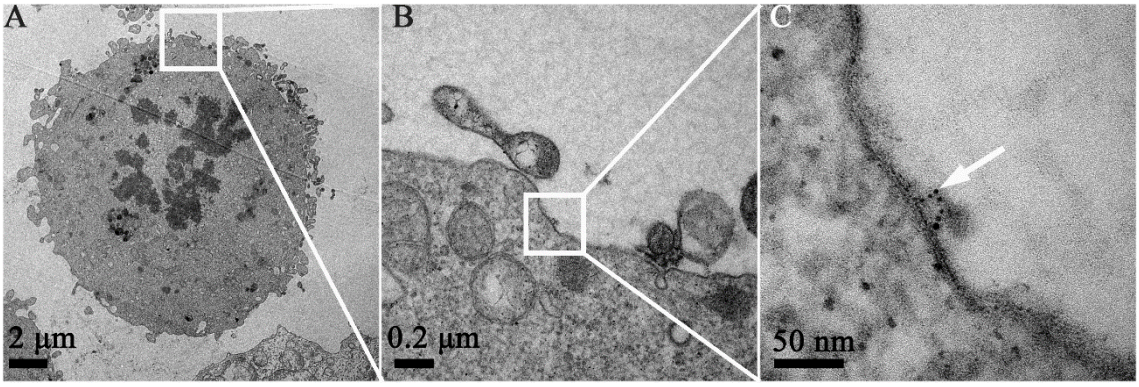

Fig. S13. TEM images of the anti-EGFR Goldbody bound onto the membrane of HeLa cell. White arrows indicate the anti-EGFR Goldbody, while the potential out-of-membrane parts of EGFR are visible.

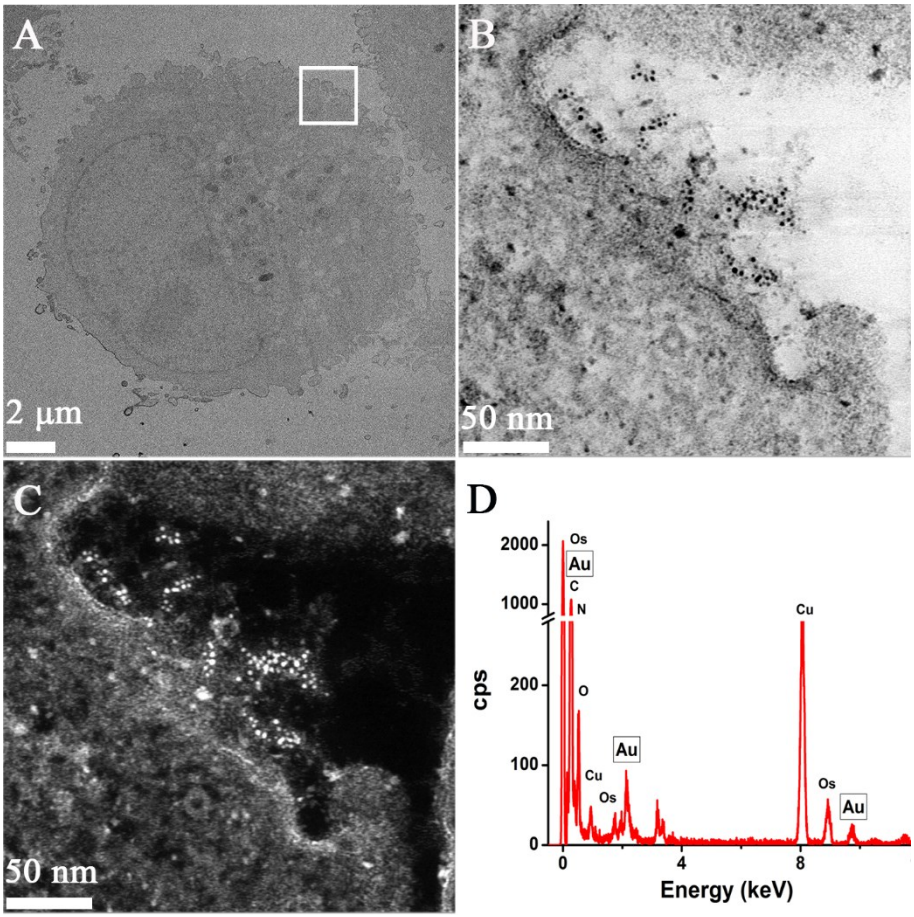

Fig. S14. HRTEM images and EDS analysis of the anti-EGFR Goldbody bound onto the membrane of HeLa cell. **(B)** and **(C)** are the bright field **(B)** and dark field **(C)** amplifications of the square in **(A)**. **(D)** shows the EDS result of the square in **(A)**.

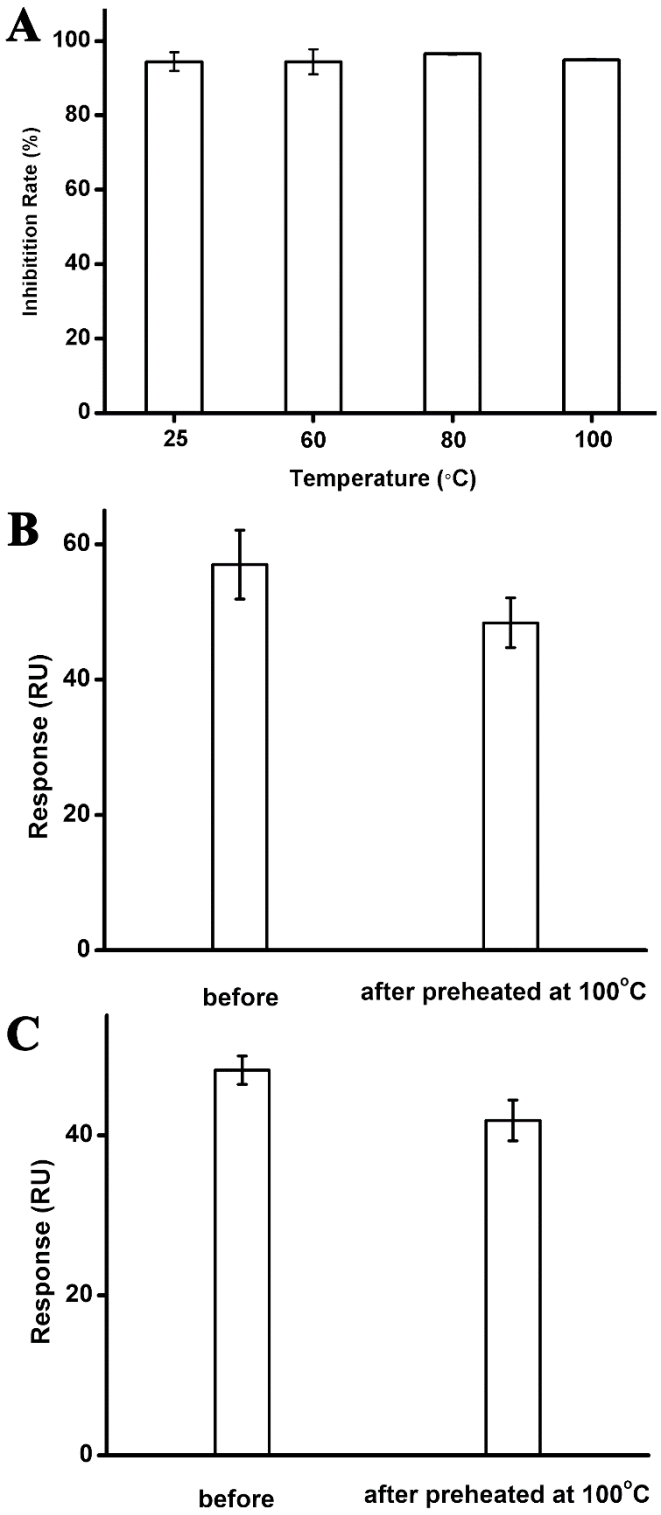

Fig. S15. Thermal stability of Goldbodies. **(A)** Inhibition of the activity of HEWL by the anti-lysozyme Goldbody (AuNP-Pep1) that had been pre-heated for 1 h at different temperatures**. (B)** SPR binding of the anti-lysozyme Goldbody (before and after preheated for 1h) to the immobilized HEWL**. (C)** SPR binding of the anti-EGFR Goldbody (before and after preheated for 1h) to the immobilized sEGFR.